

# Rheology and fuel properties of slurries of char and bio-oil derived from slow pyrolysis of cassava pulp residue and palm shell

Chaiyot Tangsathitkulchai\*<sup>†</sup>, Piyarat Weerachanchai\*, and Malee Tangsathitkulchai\*\*

\*School of Chemical Engineering, \*\*School of Chemistry,  
Suranaree University of Technology, Muang District, Nakhon Ratchasima 30000, Thailand  
(Received 31 August 2011 • accepted 28 March 2012)

**Abstract**—Three bio-oil samples, namely, raw bio-oil from pyrolysis of cassava pulp residue (CPR), separated oil phase and aqueous phase of bio-oil from pyrolysis of palm shell (PS), were used as suspending media for preparing slurries of bio-oil and the co-product char. Rheologies of all tested slurries exhibited pseudoplasticity with yield stress and the degree of this non-Newtonian behavior depended on such parameters as slurry type, solid concentration, particle size and slurry temperature. Overall, char/bio-oil slurries gave better fuel properties including higher pH and reasonably high calorific value (18-32 MJ/kg) as compared to their bio-oil properties. Combustion of char/bio-oil slurries occurred in the temperature range similar to their solid char combustion and without ignition delay.

Key words: Bio-oil, Biomass, Char, Slurry Rheology, Pyrolysis

## INTRODUCTION

Bio-oil, a liquid product from the pyrolysis of biomass, has been recognized as a promising renewable energy source, due principally to its ease of handling, storage and transportation. Its commercial use has been reported with some success when burned in existing furnace systems or co-fired with other types of fuels [1,2]. However, bio-oil possesses inherent drawbacks of corrosiveness, high water content, chemical instability and relatively low heating value, resulting mainly from its containing a large number of different chemical species especially the oxygenated compounds [3,4]. Several methods have been proposed to improve these undesirable properties of bio-oil, for example, the removal of oligomeric molecules by hot-vapor filtration, conversion of acid contents by chemical/catalytic upgrading, etc. [5-7]. The complex chemical constituents in bio-oil coupled with the low yield of derived upgraded oil and high costs of chemical recovery have hampered the full development of the oil upgrading processes.

In this work, we propose a simple approach aimed to increase specifically the low heat content of bio-oil containing relatively large amount of water by mixing the bio-oil with its char product to form a slurry fuel that still maintains the flow character of liquid oil. Basic rheological properties of char/bio-oil slurries, which are of prime importance for the design of slurry transport through pipeline and spray nozzles, are measured with a coaxial bob-and-cup viscometer as a function of solid concentration, particle size and slurry temperature. Some fuel properties and basic combustion characteristics of the fuel mixtures are also determined.

## EXPERIMENTAL

### 1. Raw Materials

The chars and bio-oils used for the rheological study were obtained

from the slow pyrolysis of two potential biomasses, cassava pulp residue (CPR) and palm shell (PS), which are solid wastes discarded from tapioca flour mills and palm-oil refining factories, respectively. Each biomass with the average screen size of 2.03 mm was heated in a tubular fixed-bed reactor from room temperature, at the heating rate of 20 °C/min under a constant flow of N<sub>2</sub> (200 cm<sup>3</sup>/min), to the final temperature of 700 °C and held for one hour to complete the devolatilization process. Details of the experimental procedure for the biomass pyrolysis are reported elsewhere [8].

Bio-oil collected from the pyrolysis of cassava pulp residue showed an appearance of a homogeneous transparent phase with dark red-brown color, whereas that derived from palm shell gave a dispersion of oil phase in an aqueous solution phase. These two liquid phases of palm shell bio-oil were then separated by centrifuging at 3,000 rpm for 30 min. All bio-oil samples were finally filtered to remove the residual char and then stored in a refrigerator prior to the rheological measurement.

### 2. Material Characterization

Three different bio-oil samples were used as suspending media for slurry preparation: raw bio-oil from cassava pulp residue, and the separated oil phase and aqueous solution of bio-oil from palm shell. They were analyzed for the following fuel properties: calorific value (ASTM D240-920), density (Gay-Lussac bottle), viscosity (ASTM D445-96), carbon residue (ASTM D524-97), ash content (ASTM D482-95), and pH (744 pH meter, Metrohm). Water contents in the raw bio-oils of cassava pulp residue and palm shell were determined by refluxing both oils with toluene solution using the Dean-Stark method (ASTM D95-83).

The char products from pyrolysis of the two biomasses (CPR and PS) were characterized for their physicochemical properties. The physical properties measured were bulk density, true density (He pycnometer, Accupyc 1330, Micromeritics), calorific value (ASTM D3286-96), particle size distribution (laser diffraction size analyzer, Mastersizer S, Mavem), and porous properties (surface area analyzer, ASAP2010, Micromeritics). Proximate analysis (moisture content

<sup>†</sup>To whom correspondence should be addressed.  
E-mail: chaiyot@sut.ac.th

(ASTM D2867-95), volatile content (ASTM D5832-95), ash content (ASTM D2866-94) and fixed carbon (by mass balance), elemental analysis (CHNS/O analyzer, Perkin Elmer PE2400 series II) were determined for the chemical compositions.

Basic fuel properties of the test slurries were determined by using the same measurement methods as those of suspending bio-oils. In addition, the combustion behaviors of bio-oils, chars and char/bio-oil slurries were investigated by following the sample weight loss on combustion in air as a function of increasing heating temperature by using a thermogravimetric analyzer (SDT 2960 DSC-TGA model, TA Instruments).

### 3. Rheological Measurement

Rheological characteristics of char/bio-oil slurries were measured with a Haake VT550 concentric cylinder viscometer. Two sensors of NV and SV-I were used for the low and high viscosity range measurements, respectively. The cylindrical system of NV sensor type has a cup-to-bob radius ratio of 1.02 mm and the bob radius of 20.1 mm and those of SV-I system are 1.14 and 10.1 mm, respectively. The rheological properties of slurries prepared under differing conditions were determined under laminar flow conditions covering shear rates ranging from  $0.712\text{--}690\text{ s}^{-1}$  (0.8–775 rpm). During measurement, the slurry was maintained at a constant temperature by circulating water from a refrigerated bath through the jacket of temperature vessel of the viscometer. Table 1 lists the experimental con-

ditions used for the rheological measurement.

## RESULTS AND DISCUSSION

### 1. Raw Material Properties

Basic physical and fuel properties of suspending bio-oils used for slurry preparation are listed in Table 2. Among the three suspending bio-oils, the raw bio-oil from CPR gives the lowest values of density and viscosity,  $1.09\text{ g/cm}^3$  and  $2.94\text{ cSt}$ , respectively. The oil phase of palm shell bio-oil shows a much greater viscosity ( $23.39\text{ cSt}$ ) than that of its aqueous phase ( $3.48\text{ cSt}$ ), although their densities are quite comparable. It is noted that all the test bio-oils exhibit relatively low pH varying in the range of 2.95–3.21, due largely to the presence of various oxygenated compounds such as organic acids and phenols [9,10]. The raw bio-oil from CPR contains relatively high water content of 56.41 wt%. Calorific values of raw bio-oil from CPR and the aqueous phase of PS bio-oil cannot be directly measured, whereas a moderate heating value of  $25.55\text{ MJ/kg}$  is achievable with the oil phase of PS bio-oil. Further, the oil phase of PS bio-oil provides the largest values of Ramsbottom carbon residue (6.35 wt%) and ash content (0.089 wt%).

Physicochemical properties of pyrolysis chars are given in Table 3 and their particle size distributions in Fig. 1, with volume-surface mean diameter ( $D_{32}$ ) being listed in Table 3. The CPR char and PS char give relatively similar true density values, whereas the bulk

**Table 1. Conditions used for rheological measurement of char/bio-oil slurries**

Parametric effect	Slurry concn. (wt% solid)	Particle size ( $\mu\text{m}$ )	Slurry temp. ( $^{\circ}\text{C}$ )
Slurry type			
CPR char+raw oil	30	–38	25
CPR char+water	30	–38	25
PS char+oil phase	30	–38	25
PS char+aqueous sol.	30	–38	25
Slurry concentration			
CPR char+raw oil	10, 25, 30, 35, 40	–38	25
PS char+oil phase	30, 40	–38	25
Particle size			
CPR char+raw oil	30	–38, –75, –106	25
Temperature			
CPR char+raw oil	30	–38	15, 25, 35, 45

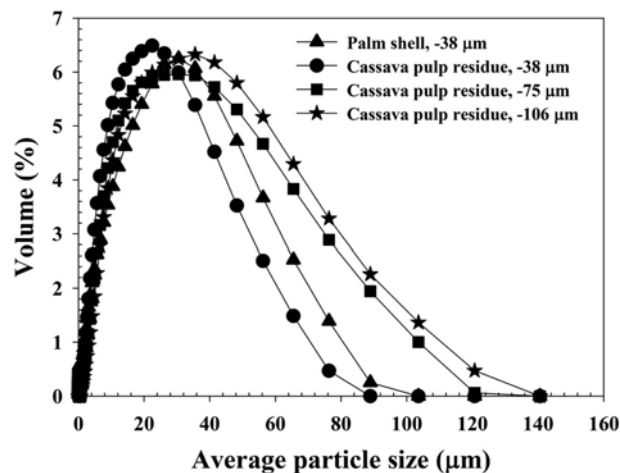


**Fig. 1. Particle size distributions of test chars for slurry preparation.**

**Table 2. Properties of bio-oils and water used for rheological study**

Properties	Cassava pulp residue		Palm shell		Water
	Raw bio-oil	Raw bio-oil	Oil phase phase	Aqueous	
Density ( $\text{g/cm}^3$ ) at $25\text{ }^{\circ}\text{C}$	1.09	1.11	1.13	1.10	1.02
Viscosity (cSt) at $25\text{ }^{\circ}\text{C}$	2.94	4.75	23.39	3.48	1.02
pH	2.95	2.98	3.21	2.95	6.88
Calorific value (MJ/kg)	*	*	25.55	*	-
Ramsbottom carbon residue (wt%)	2.57	2.93	6.35	2.88	-
Ash content (wt%)	0.081	0.071	0.089	0.063	-
Water content (wt%)	56.41	48.78	**	**	-

\*Unmeasurable, \*\*Not analyzed

**Table 3. Properties of solid chars used for slurry preparation**

Properties		CPR char		PS char
True density (g/cm <sup>3</sup> )		1.754		1.689
Bulk density (g/cm <sup>3</sup> )	0.588	0.556	0.535	0.801
Particle size (μm)	-38	-75	-106	-38
Volume-surface mean diameter, D <sub>32</sub> (μm)	8.2	11.1	12.5	2.4
Calorific value (MJ/kg)	29.28	33.36		
Proximate analysis (wt%) (dry basis)				
Volatile matter		29.23		12.66
Fixed carbon		56.36		82.11
Ash		14.41		5.23
Elemental analysis (wt%)				
C		55.28		79.31
H		1.66		2.66
O		42.47		17.99
N		0.57		-
S		0.02		0.04
H/C		0.36		0.40
O/C		0.57		0.17
Porous properties				
BET surface area (m <sup>2</sup> /g)		34		367
Micropore volume (cm <sup>3</sup> /g) (%)		0.013(59.1)		0.155(87.1)
Total pore volume (cm <sup>3</sup> /g)		0.022		0.178
Average pore size (nm)		2.58		2.14

density of PS char is significantly larger than that of CPR char for the same particle size of smaller than 38 μm. In addition, for CPR char there is a tendency for the bulk density to slightly increase when the particle size distribution becomes narrower (smaller mean particle size). On the chemical composition analysis, CPR char has higher volatile content, ash content and O/C ratio but much lower fixed carbon in comparison with PS char. For the porous characteristics, PS char which has smaller average pore size gives much higher BET surface area and total pore volume as well as higher percentage of micropore volume than those of CPR char.

## 2. Rheological Properties

Fig. 2 shows typical responses of shear stress as a function of measuring time when the slurry was sheared at a constant rotor speed.

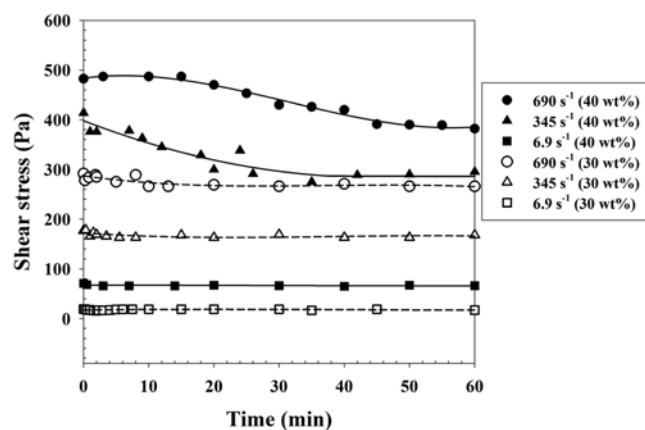


**Fig. 2. Effect of shearing time on shear stress for CPRchar/bio-oil slurries (-38 μm, 25 °C).**

At low solid concentration of 30 wt% and shear rates smaller than 345 s<sup>-1</sup>, the shear stress remains substantially constant independent of shearing time. However, at higher shear rate of 690 s<sup>-1</sup>, a slight decrease in the shear stress is observed for the first 5 min of shearing time before attaining a constant value at longer times. At higher solid loading of 40 wt%, where particles are getting closer, the drop in the shear stress occurs at a lower shear rate of 345 s<sup>-1</sup> compared to the case of 30 wt% slurry, and the time required to achieve a steady shear stress is longer as the shear rate is increased. The observed variation of shear stress with the time of shearing is believed to result from the breakdown and realignment of some agglomerates in the slurry due to the cohesive force of fine particles [11]. High shearing rate on a slurry with high solid concentration requires longer time for restructuring solid particles in the direction of flow. It should be noted that all reported shear stresses for rheological study of char/bio-oil slurries in this work are the final steady-state values. No attempt was made at this stage to examine the time-dependent rheological behavior of these slurries.

In this study, the rheological behavior of all test slurries was found to be best described by a power-law model with yield stress or Herschel-Bulkley model [12],  $\tau = \tau_0 + K\dot{\gamma}^n$ , where  $\tau$  is the shear stress (Pa),  $\tau_0$  is the yield stress (Pa),  $\dot{\gamma}$  is the shear rate (s<sup>-1</sup>), and K and n are the consistency index and flow index, respectively. The consistency index reflects the viscous nature of the slurry, whereas the flow index indicates the degree of deviation from Newtonian flow character (n<1, pseudoplastic and n>1, dilatant). Table 4 summarizes the fitted rheological parameters of char/bio-oil slurries studied in this work.

### 2-1. Effect of Slurry Type

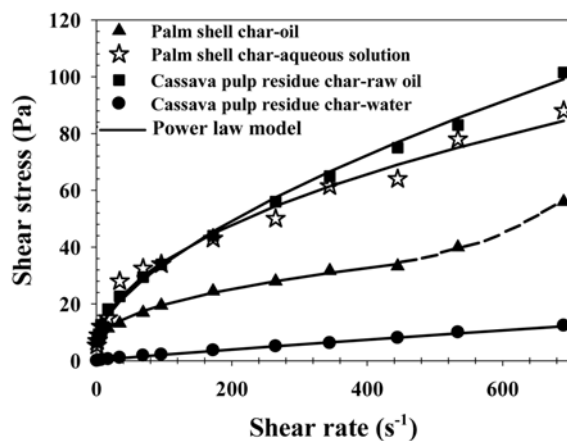
Four different slurry systems prepared by a combination of dif-

**Table 4. Fitted values of power-law model parameters for various test slurries**

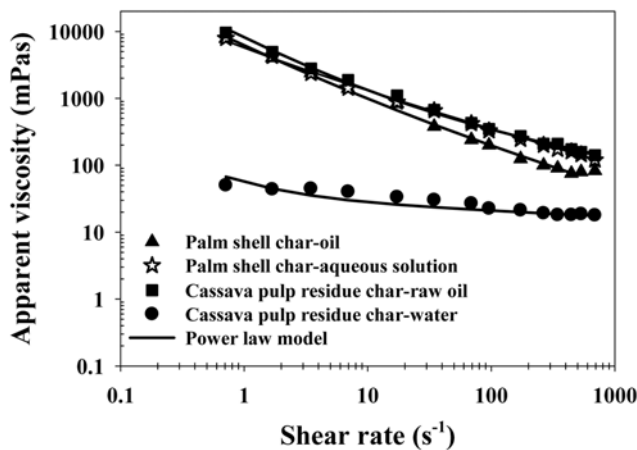
Parametric effect	$\tau_0$ (Pa)	K	n
Slurry type (25 °C, -38 $\mu$ m, 30 wt% solid)			
CPR char+raw oil	6.61	1.56	0.625
CPR char+water	0.025	0.032	0.910
PS char+oil phase	4.06	2.14	0.432
PS char+aqueous sol.	1.92	3.78	0.472
Slurry concentration (wt% solid) (CPR char+raw oil, 25 °C, -38 $\mu$ m)			
10	0.233	0.028	0.837
25	2.88	0.150	0.740
30	6.61	1.56	0.625
35	8.01	1.90	0.702
40	40.0	7.27	0.5
(PS char+oil phase, 25 °C, -38 $\mu$ m)			
30	4.06	2.14	0.472
40	9.03	0.004	2.39
Particle size ( $\mu$ m) (CPR char+raw oil, 25 °C, 30 wt% solid)			
-38	6.61	1.56	0.625
-75	4.88	1.42	0.690
-106	4.83	1.20	0.747
Temperature (°C) (CPR char+raw oil, -38 $\mu$ m, 30 wt% solid)			
15	7.97	1.36	0.668
25	6.61	1.56	0.625
35	5.15	1.24	0.614
45	2.39	1.68	0.576

ferent chars and suspending media were employed to examine the rheological dependence on the nature of slurry type, using conditions of 30 wt% solid, -38  $\mu$ m particle size and at 25 °C. Results in Fig. 3 indicate that the four types of test slurries display non-Newtonian pseudoplastic behavior (decreasing slurry viscosity with increasing the rate of shearing) with varying degrees of pseudoplasticity as observed from the rheological parameters in Table 4. CPR char-water slurry exhibits the rheological character close to a Newtonian fluid with the flow index (n) of 0.91 and a very low yield stress, while the rest of char/bio-oil slurries give the value of n varying from 0.43-0.62 with CPR char-oil slurry giving the largest yield stress of 6.61 Pa. This pseudoplastic flow behavior is commonly found in many other different solid slurries, including coal-water slurries [13-15], mineral-water slurries [16,17], coal-oil mixtures [18,19] and coal-water-oil slurries [20].

In principle, if the solid and suspending liquid are both inert, the apparent viscosity of a slurry should be directly proportional to the medium viscosity [21]. This means that the relative apparent viscosity of the slurry, defined as the ratio of slurry viscosity ( $\mu_s$ ) and medium viscosity ( $\mu_t$ ), must remain constant. However, it is clear from Fig. 4 that this criterion is not met at least with the slurries studied in this work, that is, discrepancies exist between slurries of PS char-oil phase vs. PS char-aqueous phase and between slurries of CPR char-oil vs. CPR char-water. This anomaly could result from the effect and role of various chemical constituents present in the bio-



(a)



(b)

**Fig. 3. Shear stress and apparent viscosity of various test slurries as a function of shear rate (30 wt% solid, -38  $\mu$ m, 25 °C).**

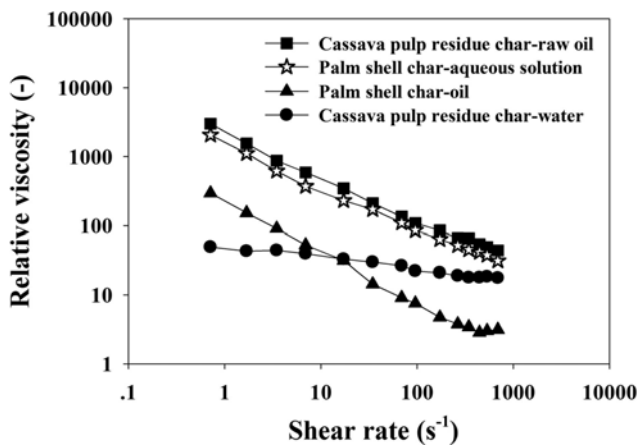


**Fig. 4. Relative apparent viscosity of various slurries as a function of shear rate.**

oil since there was evidence of increased viscosities for slurries prepared from coal and low-viscosity organic solvents such as cyclohexane and alcohols, as compared to coal-water slurry systems under the same rheological conditions [22]. Although using bio-oil as a suspending medium appears to give higher stress and viscosity than

using water, it offers certain advantage of providing better slurry stability. For example, we found that on standing the CPR char-water slurry at 30 wt% solid gave complete particle sedimentation within 5 hours, while it took about 72 hours for CPR char/bio-oil slurry at the same solid concentration to attain the final sedimentation state. Further examination of Fig. 3(a) reveals a peculiar result for PS char-oil phase slurry at 30 wt% solid. It displays pseudo-plastic flow behavior up to a critical shear rate of  $445 \text{ s}^{-1}$ , followed by dilatant or shear-thickening behavior at higher shear rates. This is not expected since the dilatancy effect (increasing flow resistance with increasing shear rate) is generally associated with highly concentrated suspensions where particles are densely packed [11,23]. It is probable that the observed dilatant flow behavior could be connected to the much higher viscosity of oil phase of PS char slurry (23.39 cSt), but the exact mechanism for this behavior is not clearly understood.

## 2-2. Effect of Solid Concentration

Obviously, the highest energy content of char/bio-oil slurry is determined by the maximum solid loading that still permits the flow of slurry. In this work, the effect of solid concentration was investigated for CPR char-raw oil slurries in the range from 10 to 40 wt% solid and for PS char-oil slurries at 30 and 40 wt% solid, for  $-38$

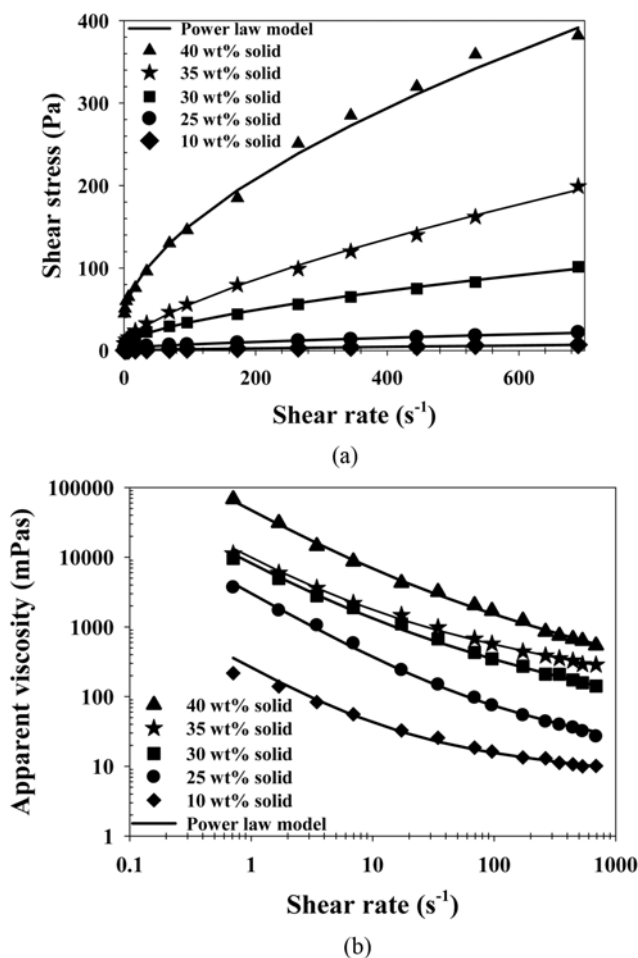


Fig. 5. Effect of solid concentration on shear stress and apparent viscosity of CPR char-oil slurry as a function of shear rate ( $-38 \mu\text{m}$ ,  $25^\circ\text{C}$ ).

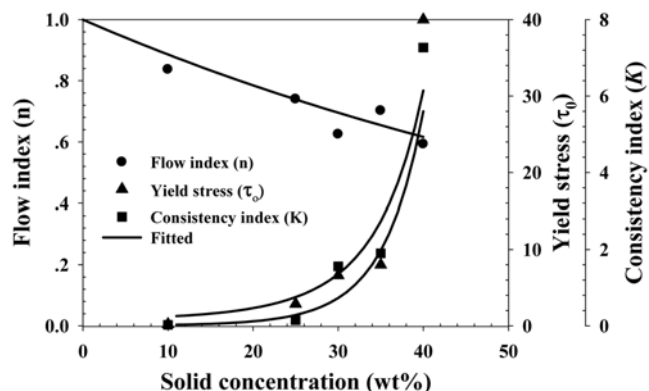


Fig. 6. Effect of solid concentration on rheological parameters of the power-law model (CPR char-oil slurries,  $-38 \mu\text{m}$ ,  $25^\circ\text{C}$ ).

$\mu\text{m}$  particle size and at  $25^\circ\text{C}$ . Rheological results as shown in Fig. 5 and Table 4 indicate that CPR char/bio-oil slurries exhibit pseudo-plastic flow behavior with continued increasing of yield stress and decreasing of flow index (more deviation from Newtonian flow), as the slurry concentration is increased. Fig. 6 further shows the dependence of the three rheological parameters on solid concentration. It illustrates an abrupt increase of yield stress and consistency index from 35 to 40 wt% solid. This indicates that particle interaction (frictional effect) becomes much more pronounced when maximum packing of particles is approached, which is reflected by a very high viscosity of the slurry at 40 wt% solid ( $\sim 2,000 \text{ mPas}$  at  $100 \text{ s}^{-1}$  shear rate). Thus, the judicious selection of a suitable solid concentration should be based on a balance between an increase in energy content due to increased char loading and an increase in the flow resistance of slurry, which means the increase in pumping cost for slurry transport. Empirical equations are proposed for estimating  $\tau_0$ , K and n as a function of solid weight fraction ( $\phi=0-0.4$ ) for CPR char/bio-oil slurries as follows.

$$\text{For yield stress: } \tau_0 = \exp[21.8\phi^{2.02}] \quad (1)$$

$$\text{For consistency index: } K = 0.01 \exp[21.8\phi^{1.35}] \quad (2)$$

$$\text{For flow index: } n = \exp[-1.21\phi], \quad (3)$$

For the case of PS char-oil slurries, Fig. 7(a) indicates that in general the 40 wt% solid slurry exhibits dilatant flow behavior and can be well fitted by the power-law model over the narrow range of measuring shear rate ( $0-320 \text{ s}^{-1}$ ), with the flow index (n) of 2.39. At lower solid concentration of 30 wt% solid, the slurry shows pseudo-plastic behavior up to the shear rate of  $445 \text{ s}^{-1}$  with the flow index of 0.432 and dilatant behavior at shear rates from 445 to  $650 \text{ s}^{-1}$ , as discussed earlier. However, closer examination of calculated apparent viscosity as a function of shear rate, as shown in Fig. 7(b), reveals that the 40 wt% solid slurry also shows pseudo-plastic behavior, but over a low and narrow range of shear rates smaller than  $50 \text{ s}^{-1}$ , followed by dilatant behavior at higher shear rates. This flow behavior also occurs for the 30 wt% solid slurry, but the critical shear rate at which pseudo-plasticity transforms to dilatancy shifts to a larger value of shear rate at  $445 \text{ s}^{-1}$ , as observed earlier. From these limited data, it may be argued that, for PS char-oil phase slurry, there is a flow transition from true pseudo-plasticity at a very low solid concentration to true dilatancy at a very high solid concentration. Between

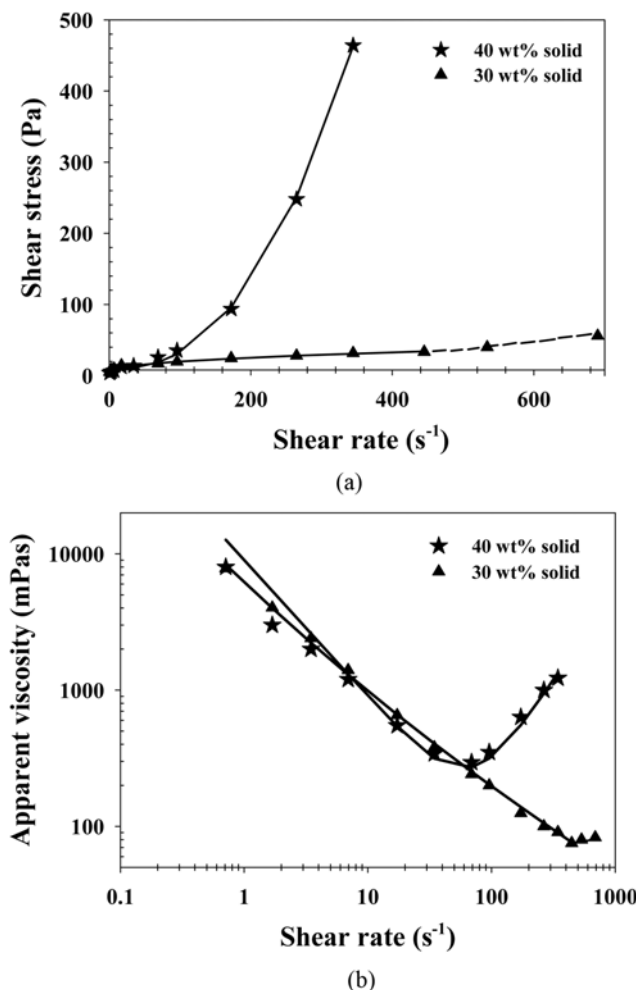


Fig. 7. Shear stress and apparent viscosity of PS char-oil phase slurry as a function of shear rate at 30 and 40 wt% solid (-38 μm, 25 °C).

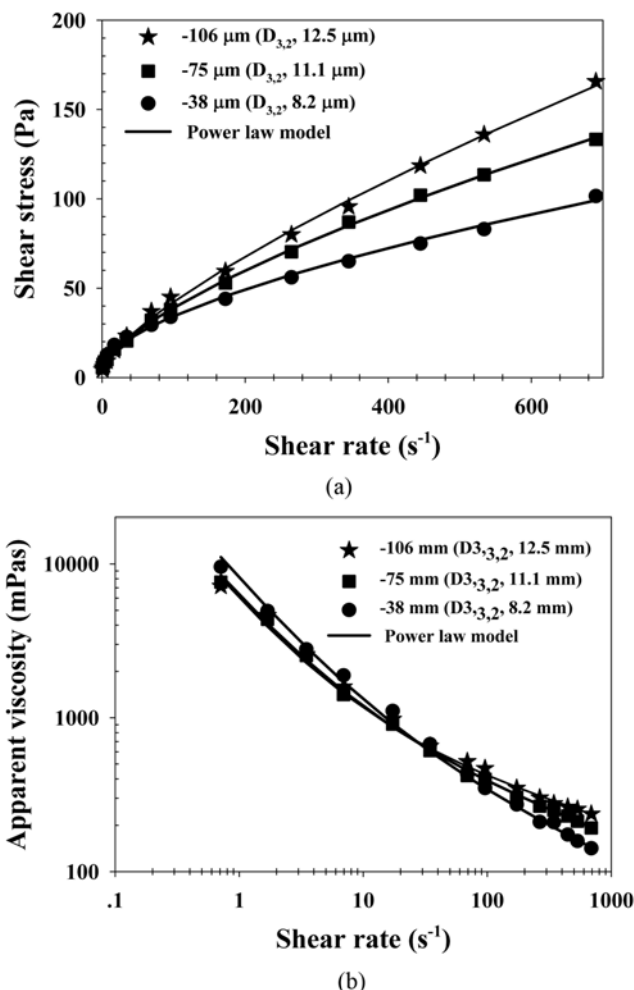


Fig. 8. Effect of particle size on shear stress and apparent viscosity of CPR char-oil slurry as a function of shear rate (30 wt% solid, 25 °C).

these two limiting concentrations, the flow character can display either pseudoplastic or dilatant behavior, depending on the range of shear rate and this in turn is primarily determined by the slurry concentration. Concerning this flow behavior, the use of PS char-oil slurry as a burning fuel may cause a problem of pump and injector blockage and probably poor atomization when operating at a very high shear rate or at a high slurry concentration. In this case, a chemical additive, which acts as a particle dispersing agent, may be required to alter the rheological behavior or effectively lower the slurry viscosity [15,24].

2-3. Effect of Particle Size

CPR char with three particle size distributions of -38, -75 and -106 μm, corresponding to volume-surface mean diameter of 8.2, 11.1 and 13.0 μm, respectively, were employed for rheological measurement of char-raw oil slurries at 30 wt% solid and at 25 °C. Rheological results shown in Fig. 8(a) indicate that the three test slurries exhibit pseudoplastic flow behavior and the flow curves appear to systematically shift upward as the mean particle size is increased. As Table 4 shows, a slurry with wider size distribution (larger mean size) gives lower values of yield stress ( $\tau_c$ ) and consistency index (K) and larger flow index (n), which means that the slurry behaves

closer to Newtonian flow behavior.

There are two possible effects that particle size can influence the rheological behavior of a given slurry. The first effect is particle packing, which indicates the way smaller size particles can fill or packed in the interstices of larger particles and the second one is cohesive forces of fine particles [25,26]. The packing characteristic can be roughly traced from the slope of cumulative size distribution plot, which measures the relative mass fraction of various size ranges of large and small particles. Here, the particle size distribution in cumulative form can be well fitted with Rosin-Rammler (R-R) equation [21,27] which reads

$$P(x) = 1 - \exp[-(x/k)^m] \tag{4}$$

where P(x) represents the cumulative weight fraction of particles smaller than size x, k is the size modulus and m is the distribution modulus determined from the slope of the linear plot of P(x) versus x. On fitting the size distribution data with R-R distribution function, the following parameters are obtained:

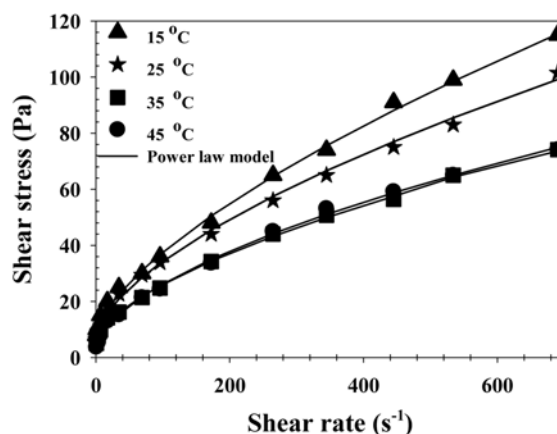
- For -38 μm fraction: k=19 μm, m=1.26
- For -75 μm fraction: k=27 μm, m=1.22

For  $-106 \mu\text{m}$  fraction:  $k=29 \mu\text{m}$ ,  $m=1.25$

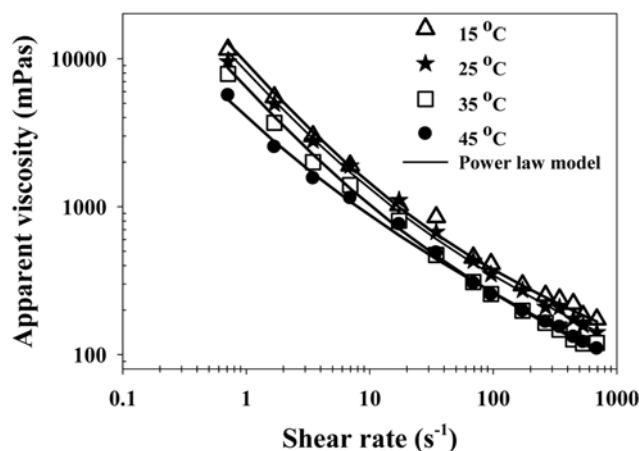
It is clear that there is almost no difference in the value of  $m$  for the three size fractions of char particles. Since packing is a function of  $m$ , it is plausible to deduce that the rheology of CPR char/raw bio-oil slurries does not primarily depend on particle packing but could be determined by cohesion of fine particles in the slurry. This reasoning is partly supported by the lowering of yield stress and consistency index when mean particle size is increased as mentioned earlier, since larger size fraction contains less fines and hence less cohesive forces among fine particles. As to the slurry viscosity, Fig. 8(b) suggests that over the high shear rate range ( $50\text{--}800 \text{ s}^{-1}$ ), the slurry containing large amount of fines (smaller mean size fraction) shows a stronger drop in slurry viscosity with reference to the increase in the rate of shear and this again confirms the role of fine particles through cohesion effect on the degree of pseudoplasticity of slurry.

#### 2-4. Effect of Slurry Temperature

The dependence of slurry rheology on temperature in the range from  $15\text{--}45 \text{ }^\circ\text{C}$  was studied using CPR char/bio-oil slurry at 30 wt% solid and particle size of  $-38 \mu\text{m}$ . As Fig. 9(a) and Table 4 show, the slurries exhibit pseudoplastic flow character with increasing degree of non-Newtonian pseudoplasticity (decreasing flow index) and lowering of yield stress as the slurry temperature is increased. This behavior should result mainly from the reduction of suspending liquid viscosity with increasing slurry temperature. Technically, it is advantageous to operate this type of slurry at a higher temperature to impart more pseudoplastic character, hence giving lowered viscosity especially at a high shear rate (Fig. 9(b)). However, increasing temperature from  $35$  to  $45 \text{ }^\circ\text{C}$  gives almost no change in the viscosity, particularly at shear rate larger than  $30 \text{ s}^{-1}$ . It is likely that some bio-oil may have evaporated during the measurement, giving a compensation effect between increased viscosity of the thick slurry and a decrease of medium viscosity as the temperature was increased.



(a)



(b)

Fig. 9. Effect of slurry temperature on shear stress and apparent viscosity of CPR char-oil slurry as a function of shear rate (30 wt% solid,  $-38 \mu\text{m}$ ).

Table 5. Some fuel properties of various test slurries

Slurry types	Density at $25 \text{ }^\circ\text{C}$ ( $\text{g}/\text{cm}^3$ )	Viscosity at $25 \text{ }^\circ\text{C}$ , shear rate @ $100 \text{ s}^{-1}$ (cSt)	Calorific value ( $\text{MJ}/\text{kg}$ )	Ash content (wt%)	pH
CPR char-raw oil, $-38 \mu\text{m}$ size with different wt% solid					
0	1.09	2.94	-	0.081	2.95
10	1.15	15.5	-	2.55	2.95
25	1.20	74.1	-	5.58	3.04
30	1.26	344	18.2	6.64	3.86
35	1.37	562	18.9	8.21	4.05
40	1.52	1520	20.3	9.22	4.27
PS char-oil phase, $-38 \mu\text{m}$ size with different wt% solid					
0	1.13	23.4	25.6	0.089	3.21
30	1.30	179	31.7	4.15	3.98
40	1.61	327	33.2	4.53	4.12
PS char-aqueous sol. ( $-38 \mu\text{m}$ size and 30 wt% solid)	1.29	351	17.9	3.85	3.54
CPR char-water ( $-38 \mu\text{m}$ size and 30 wt% solid)	1.16	21.4	-	5.61	10.6

This reasoning was checked by running the measurement at 50 °C, and it was found that the measured stress increased markedly with the depletion of slurry volume as the measuring time progressed. As a result, it is suggested that the maximum allowable temperature for operating this type of slurry should not exceed 45 °C. An attempt was also made here to correlate the dependence of yield stress on temperature in the range from 15 to 35 °C through the Arrhenius type of equation in the form:

$$\tau_0 = \tau_\infty \exp[E/RT] \quad (5)$$

where  $\tau_0$  is the yield stress in Pa,  $T$  is temperature in K,  $\tau_\infty$  is pre-exponential factor or the yield stress at  $T=\infty$ ,  $E$  is activation energy in kJ/kg-mol and  $R$  is gas constant (8.314 kJ/kg mol-K). By linear regression analysis, the values of  $\tau$  and  $E$  were found to be  $9.62 \times 10^{-3}$  Pa and  $1.61 \times 10^4$  kJ/kg-mol, respectively.

### 3. Fuel and Combustion Properties of Test Slurries

Table 5 shows some basic fuel properties of different char/bio-oil slurries. As expected, all fuel properties including density, viscosity, calorific value and ash content as well as the pH value are found to increase with increasing char loading. Thus, incorporating solid char into bio-oil to form a slurry mixture is an easy way to improve the quality of bio-oil in terms of heat content and acidity. Increasing slurry density from 30 to 40 wt% solid gives a drastic increase in slurry viscosity, but with only about 5 and 12% increase in the heating value for PS char-oil slurry and CPR char-oil slurry, respectively. It is noted that the heating value of CPR char-oil slurry can be measured only when solid concentration is greater than 30 wt%, while it is not possible to determine the heating value of CPR char-water slurry at the same solid concentration. Among various slurries, PS char-oil slurry at 30 wt% solid appears to be the best choice as a slurry fuel, judging from its reasonably high heating value of 31.7 MJ/kg and acceptable intermediate viscosity of 179 cSt at  $100 \text{ s}^{-1}$  shear rate.

Combustion characteristics of bio-oils and solid chars as detected by TGA are displayed in Figs. 10(a) and 10(b), respectively. As Fig. 10(a) shows, at 120 °C approximately 80% by weight of raw bio-oil from cassava pulp residue has devolatilized, followed by a subsequent slow devolatilization at higher temperatures, which is complete at around 600 °C. In comparison, at the same heating temperature of 120 °C, only 40 wt% of palm shell oil (oil-phase fraction) is devolatilized and shows an exothermic decomposition at higher temperature over the range from 400–540 °C. These results indicate that bio-oil from cassava pulp residue contains mainly water and light oxygenated compounds, whereas palm shell oil phase consists of oxygenated compounds and high molecular weight compounds of hydrocarbons which can combust with air. For char combustion (Fig. 10(b)), PS char gives wider range of combustion temperature compared to the combustion of CPR char (320–500 °C vs. 320–450 °C). Moreover, the maximum temperature difference of PS char is observed to be higher than that of CPR char (1.3 vs. 1.0 °C/mg) and this should result from the higher heating value of PS char, thus giving larger heat release upon combustion. The combustion behaviors of both slurries can be observed from the temperature difference curves, as shown in Fig. 10(c). CPR char-raw oil slurry presents two regions of thermal decomposition, including endothermic decomposition over the temperature 25–120 °C followed by exothermic decomposition at 300–450 °C, corresponding mainly to the combustion of

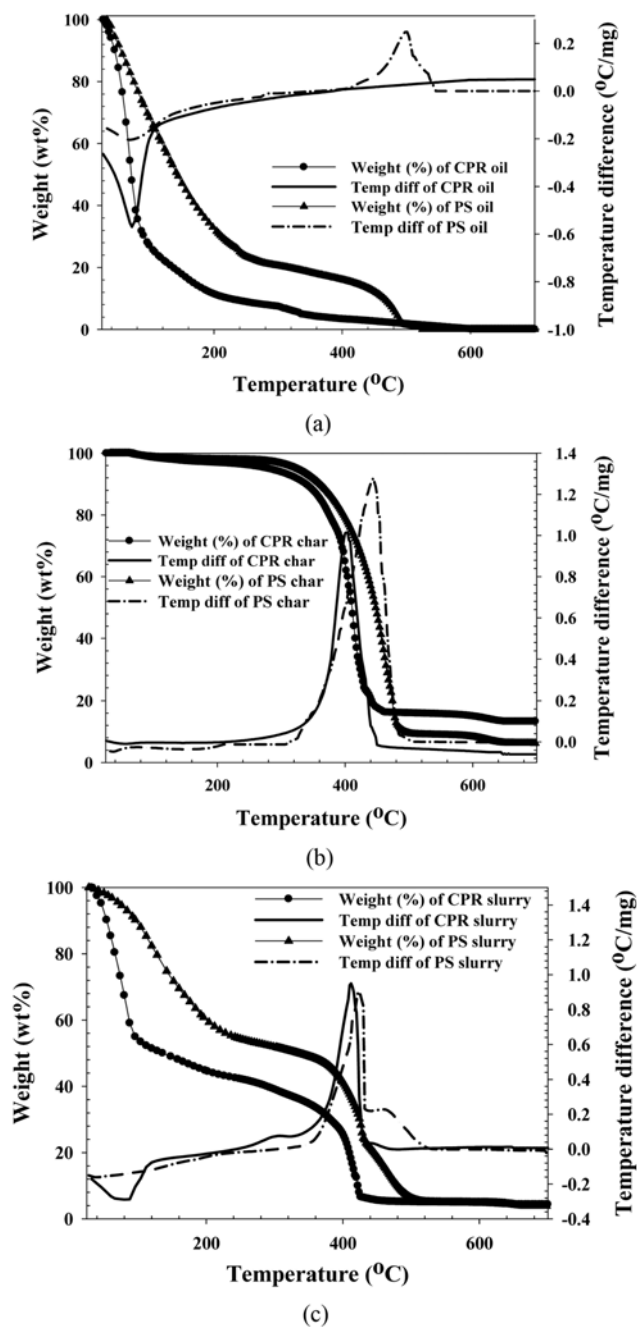


**Fig. 10.** Residual weight and temperature difference analyzed by TGA during combustion in air of (a) bio-oils, (b) solid chars, and (c) char/bio-oil slurries.

solid char. On the other hand, combustion of PS char-oil slurry exhibits one peak region with a small shoulder resulting from simultaneous combustion of bio-oil and char, covering the temperature range from 320–550 °C. As to the temperature difference curves (DTG curves), it is further noted that these two slurries show similar combustion ranges without ignition delay in comparison with their char combustion. In addition, when compared with coal-water slurries [22], the combustion of these slurries appears to give narrower peaks of DTG curves. This is indicative of faster combustion rate, hence giving complete combustion of slurry in a relatively short time period.

## CONCLUSIONS

The time-independent rheologies of char/bio-oil slurries derived from slow pyrolysis of cassava pulp residue (CPR) and palm shell (PS) were found to be well fitted by the power-law model with yield stress. Both CPR char-raw oil and PS char-aqueous phase slurries showed rheological characteristics of pseudoplastic or shear-thinning behavior-decreasing slurry apparent viscosity with increasing in the rate of shear. PS char-oil phase slurry, however, gave the flow transition from pseudoplastic to dilatant behavior at a certain shear rate. For CPR char-oil slurry, the increase of solid concentration from 10 to 40 wt% gave rise to the increase in slurry viscosity with an abrupt increase occurring in the range from 35 to 40 wt% solid. For PS char-oil slurry, increasing slurry concentration from 30 to 40 wt% solid shifted the critical shear rate, at which pseudoplastic changed to dilatant behavior, to occur at a much lower value. Wider size distribution or larger mean size of char particles gave higher shear stress and apparent viscosity at a given shear rate, but showed a decrease of yield stress and consistency index and an increase of flow index of the flow model parameters. There was a tendency for both shear stress and slurry viscosity to decrease with increasing slurry temperature, and the maximum operating temperature for CPR char-raw oil slurry without excessive evaporation of liquid carrier occurred at 45 °C. Overall, fuel properties of char/bio-oil slurries improved over those of suspending bio-oil and the test slurries combusted over the temperature range of 300-550 °C similar to their corresponding char combustion with no ignition delay.

## ACKNOWLEDGEMENT

This work was supported by the Royal Golden Jubilee Ph.D. Program (RGJ) under The Thailand Research Fund (TRF) in the form of scholarship to PW.

## REFERENCES

- Dynamotive Energy Systems Cooperation 2009. Technology [Online]. Available: <http://www.dynamotive.com>.
- P. Mckendry, *Bioresour. Technol.*, **83**, 55 (2002).
- Q. Liu, S. Wang, K. Wang, Z. Luo and K. Cen, *Korean J. Chem. Eng.*, **26**, 548 (2009).
- S. C. Hang, S. C. Yeon and C. P. Hoon, *Korean J. Chem. Eng.*, **27**, 1164 (2010).
- H. J. Park, H. S. Heo, J. H. Yim, J. K. Jeon, Y. S. Ko, S. S. Kim and Y. K. Park, *Korean J. Chem. Eng.*, **27**, 73 (2010).
- A. V. Bridgwater, *Chem. Eng. J.*, **91**, 87 (2003).
- A. Oasmaa and S. Czernik, *Energy Fuels*, **13**, 914 (1994).
- P. Weerachanchai, C. Tangsathitkulchai and M. Tangsathitkulchai, *Korean J. Chem. Eng.*, **28**, 2262 (2011).
- R. He, X. Philip-Ye, B. C. English and J. A. Satrio, *Bioresour. Technol.*, **100**, 5305 (2009).
- J. L. Zheng, W. M. Yi and N. N. Wang, *Energy Convers. Manage.*, **49**, 1724 (2008).
- G. Schramm, *A practical approach to rheology and rheometry*, Gebraueder HAAKE GmbH, Karlsruhe, Germany (1994).
- A. Lachemet, D. Touil, S. Belaadi and N. Bentaieb, *J. Appl. Sci.*, **8**, 3485 (2008).
- C. Logos and Q. D. Nguyen, *Powder Technol.*, **88**, 55 (1996).
- T. Y. Gu, G. G. Wu, Q. H. Li, Z. Q. Sun, F. Zeng, G. Y. Wang and X. L. Meng, *J. China Univ. Min. Technol.*, **18**, 50 (2008).
- J. Cheng, J. Zhou, Y. Li, J. Liu and K. Cen, *Fuel*, **87**, 2620 (2008).
- M. He, Y. Wang and E. Forsberg, *Powder Technol.*, **147**, 94 (2004).
- F. N. Shi and J. J. Napier-Munn, *Int. J. Miner. Proces.*, **65**, 125 (2002).
- D. H. Guo, X. C. Li, J. S. Yuan and L. Jiang, *Fuel*, **77**, 209 (1998).
- L. Cui, L. An and H. Jiang, *Fuel*, **87**, 2296 (2008).
- S. K. Majumder, K. Chandna, D. S. De and G. Kundu, *Int. J. Miner. Process.*, **79**, 217 (2006).
- C. Tangsathitkulchai and L. G. Austin, *Powder Technol.*, **56**, 293 (1988).
- Y. J. Shin and Y. H. Shen, *Chemosphere*, **68**, 389 (2007).
- L. Lapcik, B. Lapcikova and G. Filgasova, *Colloid. Polym. Sci.*, **278**, 65 (2000).
- E. S. Mosa, A. M. Saleh, T. A. Taha and A. M. El-Molla, *Physico-chem. Probl. Mi.*, **42**, 107 (2008).
- S. M. Olhero and J. M. F. Ferreira, *Powder Technol.*, **139**, 69 (2004).
- Z. Aktas and E. T. Woodburn, *Fuel Process. Technol.*, **62**, 1 (2000).
- M. He, Y. Wang and E. Frossberg, *Int. J. Miner. Process.*, **78**, 63 (2006).